Editors' Suggestion

Determination of the Interval between the Ground States of Para- and Ortho-H_2

M. Beyer,[1,*] N. Hölsch,[1] J. Hussels,[2] C.-F. Cheng,[2,†] E. J. Salumbides,[2] K. S. E. Eikema,[2] W. Ubachs,[2] Ch. Jungen,[3] and F. Merkt[1]

[1]*Laboratorium für Physikalische Chemie, ETH Zürich, 8093 Zürich, Switzerland*

[2]*Department of Physics and Astronomy, LaserLaB, Vrije Universiteit Amsterdam, de Boelelaan 1081, 1081 HV Amsterdam, Netherlands*

[3]*Department of Physics and Astronomy, University College London, London WC1E 6BT, United Kingdom*

(Received 18 July 2019; published 16 October 2019)

Nuclear-spin-symmetry conservation makes the observation of transitions between quantum states of ortho- and para-H_2 extremely challenging. Consequently, the energy-level structure of H_2 derived from experiment consists of two disjoint sets of level energies, one for para-H_2 and the other for ortho-H_2. We use a new measurement of the ionization energy of para-H_2 [$E_1(H_2)/(hc) = 124\,417.491\,098(31)$ cm^{-1}] to determine the energy separation [118.486 770(50) cm^{-1}] between the ground states of para- and ortho-H_2 and thus link the energy-level structure of the two nuclear-spin isomers of this fundamental molecule. Comparison with recent theoretical results [M. Puchalski *et al.*, Phys. Rev. Lett. **122**, 103003 (2019)] enables the derivation of an upper bound of 1.5 MHz for a hypothetical global shift of the energy-level structure of ortho-H_2 with respect to that of para-H_2.

DOI: 10.1103/PhysRevLett.123.163002

The conservation of parity and nuclear-spin symmetry represents the basis for selection rules in molecular physics, with applications ranging from reaction dynamics to astrophysics [1–6]. Hydrogen, in its different molecular and charged forms, e.g., H_2, H_2^+, H_3, H_3^+, etc., has played a crucial role in the derivation of the current understanding of nuclear-spin symmetry conservation and violation. H_2, for instance, exists in two distinct nuclear-spin forms, called nuclear-spin isomers, with parallel ($I = 1$, ortho-H_2) or antiparallel ($I = 0$, para-H_2) proton spins. The para isomer can be isolated and stored in large amounts [7].

The restrictions on the total molecular wave function imposed by the Pauli principle allow only even (odd) rotational levels for para (ortho) H_2 and H_2^+ in their electronic ground state $X\ ^1\Sigma_g^+$ and $X^+\ ^2\Sigma_g^+$, respectively. Consequently, the spectra of ortho- and para-H_2 and H_2^+ do not have common lines and appear as spectra of completely different molecules. Linking the energy-level structures of both nuclear-spin isomers is thus extremely challenging. A significant mixing of states of ortho and para (and gerade and ungerade) character is predicted to only occur in the highest vibrational states, because the hyperfine interaction of the atomic fragments becomes dominant at large internuclear separations and decouples the two nuclear spins [8–11]. The $N^+ = 1 \leftarrow N^+ = 0(v^+ = 19)$ pure rotational transition in H_2^+ was measured with an accuracy of 1.1 MHz (2σ) by Critchley *et al.* and represents today the only experimental connection between states of ortho- and para-H_2^+ [12]. The frequency of this transition was also determined in first-principles calculations that included quantum-electrodynamics corrections and hyperfine-induced ortho-para mixing [9,11]. This connection enables one to relate the energy-level structure of ortho- and para-H_2^+ through high-level first-principles calculations [13], which have been validated by precision spectroscopy in molecular hydrogen ions [14,15].

In this Letter, we extend this connection to the entire spectrum of H_2 by determining the ionization energy of para-H_2 following the scheme illustrated in Fig. 1. Using our recent results for the ionization energy of ortho-H_2 [16,17] and the calculated energy difference between the ground states of ortho- and para-H_2^+, we determine a value for the ortho-para separation in the electronic and vibrational ground state of H_2 and thus accurately link the energy-level structure of both nuclear-spin isomers of this fundamental molecule for the first time.

As in our previous work on ortho-H_2 [16–18], we determine the ionization energy of para-H_2 through the measurement of intervals between rovibrational levels of the $X\ ^1\Sigma_g^+$ ground state, the EF and $GK\ ^1\Sigma_g^+$ excited states and high-lying Rydberg states, with subsequent extrapolation of the Rydberg series using multichannel quantum-defect theory (MQDT).

A major difficulty that arises when applying this scheme in para-H_2 is the fact that the only p Rydberg series converging to the $v^+ = 0$, $N^+ = 0$ ground state of H_2^+, the $np0_1(0)$ series [using the notation $nlN_N^+(v^+)$ [19]] of mixed Σ^+ and Π^+ character, is heavily perturbed by rotational channel interaction with the $np2_1(0)$ series and is additionally affected by predissociation into the

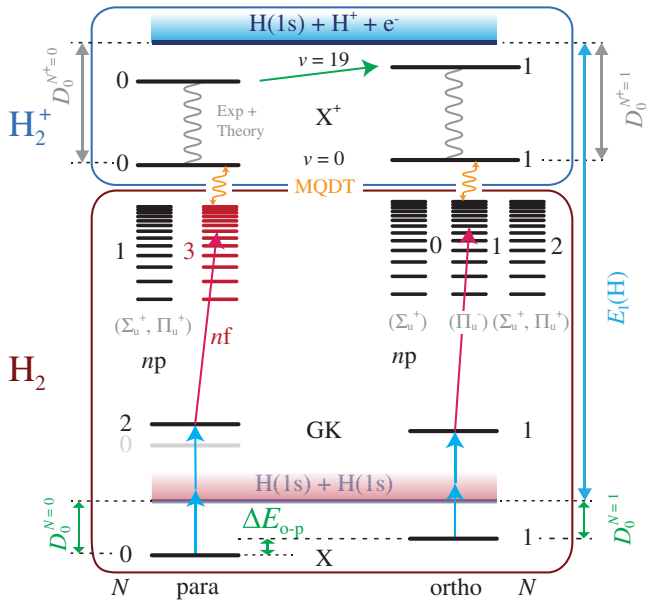

FIG. 1. Schematic diagram illustrating the energy levels and intervals of H_2 and H_2^+ (not to scale) used to determine the energy difference $\Delta E_{\text{ortho-para}}$ between the ground state of ortho- and para-H_2.

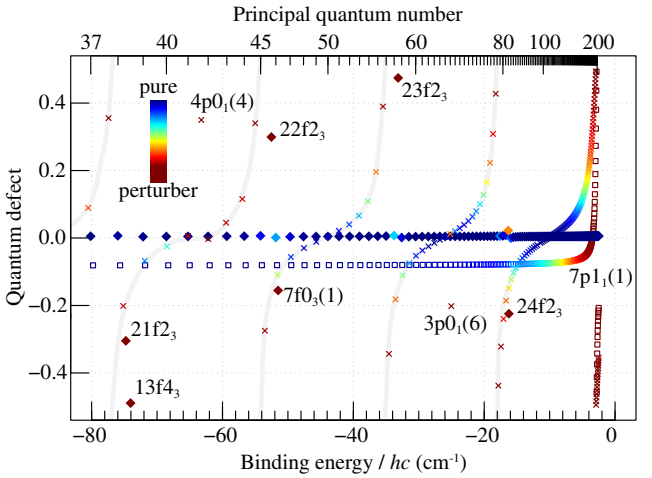

FIG. 2. Calculated effective quantum defects of the $np1_1(0)$ (open squares), $np0_1(0)$ (crosses), and $nf0_3(0)$ (full diamonds) Rydberg series. The color code indicates the character of the individual states, blue indicating an unperturbed level of series converging to $N^+ = 0$ and dark red a strongly perturbed Rydberg level with large $N^+ = 2$ character.

continuum of the $3p\sigma B'\ ^1\Sigma_u^+$ state mediated by the $3p\pi D\ ^1\Pi_u^+$ state [20,21]. In contrast, our previous determinations in ortho-H_2 [16–18,22] relied on the excitation of Rydberg states of the $np1_1(0)$ series of Π_u^- character, which is not predissociative. Moreover, there are no p Rydberg series with $N = 1$ converging on $N^+ > 1$ ionic levels in ortho-H_2, so that rotational channel interactions are strongly suppressed. In this case, perturbations can only occur by interactions with low-n Rydberg states having a vibrationally excited ion core $v^+ \geq 1$ and from weak interactions between p and f series [23]. Consequently, an MQDT extrapolation of the $np1_1(0)$ series to the ionic ground state $[X^+(v^+ = 0, N^+ = 1)]$ could be made at an accuracy of better than 150 kHz [19,23]. These considerations are illustrated in Fig. 2, which shows that the calculated effective quantum defect, $\mu = n + \sqrt{-\mathcal{R}/(\epsilon_{\text{bind}}/hc)}$, of the $np1_1(0)$ series (open squares) is indeed nearly constant for the $n < 100$ Rydberg states used in the extrapolation, and is only significantly perturbed near the ionization threshold by the $7p1_1(1)$ state ($\mathcal{R}$ is the Rydberg constant for H_2 and $\epsilon_{\text{bind}}/hc$ the Rydberg electron binding energy).

In contrast, the effective quantum defect of the $np0_1(0)$ series (crosses in Fig. 2) reveals very large perturbations with the typical divergences at the positions of the successive members of the $np2_1(0)$ series [24,25]. The extrapolation of the Rydberg series with kHz accuracy is impossible in this case because of (i) difficulties arising from the treatment of the energy dependence of the quantum defects in the MQDT framework [26] (see also Ref. [27] for a proposed solution to this problem), and (ii) the predissociation of $np0_1(0)$ Rydberg states which can shift the positions of the $n \sim 55$–75 members of the series by several MHz according to preliminary studies [28].

To overcome this problem, we choose to determine the ionization energy of para-H_2 through extrapolation of the nonpenetrating $nf0_3(0)$ Rydberg series, which is much less perturbed than the $np0_1(0)$ series. The $l(l+1)/r^2$ centrifugal barrier in the effective electron-H_2^+ interaction potential leads to a strong reduction of all nonadiabatic interactions between the electron and the ion core (i.e., predissociation and rovibrational channel interactions). The hydrogen-atom-like nature of the $nf0_3(0)$ series is illustrated in Fig. 2, which shows that the quantum defect of this series (full diamonds) is nearly zero and constant over the entire range of binding energies, allowing for a very accurate extrapolation of the ionization energy. Nonpenetrating Rydberg states have been used to derive ionization energies in more complex molecules at lower resolution (e.g., CaF [29] or benzene [30]) and to determine rovibrational intervals of molecular ions [31].

The experiments relied on the same setups and procedures as used in our recent determination of the ionization energy of ortho-H_2, and we refer to Ref. [16] for details. The $GK(1,0)$-$X(0,0)$ transition, which is two-photon allowed, turned out to be about 100 times weaker than the $GK(1,1)$-$X(0,1)$ transition of ortho-H_2, insufficient to perform a precision study. This is attributed to the lack of mixing of the $N = 0$ level with the nearby $I\ ^1\Pi_g$ state [32]. The $GK(1,2)$-$X(0,0)$ transition, probing $N = 2$, had sufficient intensity and was subjected to a precision study in Amsterdam. Frequency-comb-referenced Doppler-free

two-photon spectroscopy was performed using pulsed narrow-band vacuum-ultraviolet (VUV) laser radiation generated by nonlinear frequency up-conversion of light from a chirp-compensated injection-seeded oscillator-amplifier titanium-sapphire laser system in a BBO and a KBBF crystal. The transitions were detected by photoionizing the $GK(1,2)$ level with a separate pulsed dye laser which was delayed in time. The measurements were carried out in three campaigns distinct in time. In the first round, the Ti:sapphire laser system was pumped by a seeded Nd:YAG laser. An unseeded Nd:YAG laser was used in the other two rounds, resulting in different settings for the timing and chirp compensation.

The chirp effect on the laser pulses was counteracted by an electro-optic modulator placed inside the Ti:sapphire oscillator cavity, and the chirp of the amplified pulses was measured on-line for each pulse and used to correct the frequency. Each campaign had a different setting for the BBO- and KBBF-crystal angles and a different wavelength for the ionization laser. Therefore, ac-Stark shifts caused by the VUV and ionization lasers were measured and compensated independently in each round. Comparing the analyses of the ac-Stark effect from the 3 campaigns, the maximal error (470 kHz) was taken as the final uncertainty contribution for both VUV and ionization pulses, thus yielding a conservative estimate of this contribution to the systematic uncertainty. Possible Doppler shifts induced by nonperfectly counterpropagating VUV beams crossing the H_2 molecular beam were analyzed as in Ref. [16], by varying the velocity of the molecular beam. But instead of constraining the extrapolation to a global fit, all line positions, compensated for the ac-Stark shifts and the second-order Doppler shifts and grouped by velocity, were averaged and a residual Doppler-free value was obtained for every day. These values were averaged (see Fig. 3), yielding the Doppler-free transition frequency with an accuracy of 410 kHz. Combining this error (including statistics, residual Doppler effects, and chirp phenomena) and the major systematic uncertainties from the ac-Stark and second-order Doppler effects, the final uncertainty of the $GK(1,2)$-$X(0,0)$ interval, dominated by systematic effects, was determined to be 630 kHz, as listed in Table I.

The natural linewidth of the transitions to long-lived high-n Rydberg states is determined by the lifetime of the rovibrational level of the $GK\ ^1\Sigma_g^+$ state used as initial state. We therefore chose the $GK(0,2)$ level rather than the $GK(1,2)$ level to record the positions of the $nf0_3(0)$ series because its wave function is localized in the K outer well, leading to a threefold increase in lifetime. To combine the results of the $GK(1,2)$-$X(0,0)$ measurements carried out in Amsterdam and the $nf0_3(0)$-$GK(0,2)$ measurements carried out in Zurich, we use the relative position of the $GK(0,2)$ and $GK(1,2)$ rovibrational levels determined very accurately in Ref. [33] (see Table I).

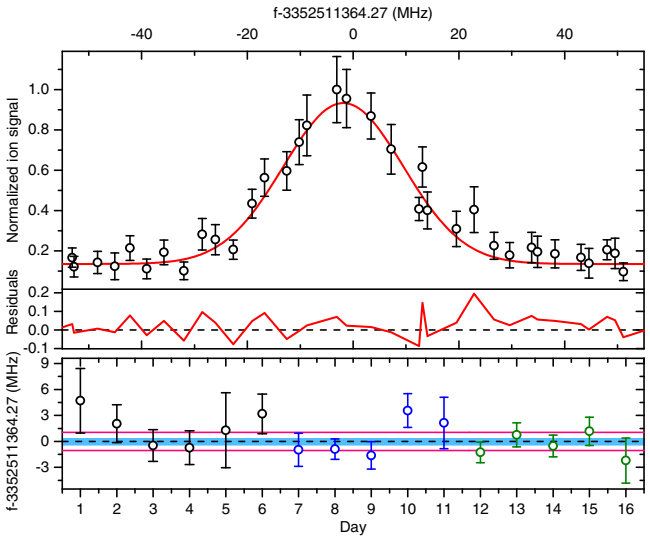

FIG. 3. Upper panel: Example of a chirp-compensated scan of the $GK(1,2)$-$X(0,0)$ line, before corrections of Stark and Doppler effects. The best fit is a Gaussian with FWHM of 27 MHz, resulting from the Fourier-transform limited bandwidth of the 25 ns laser pulse and the 30 ns lifetime of the GK state. Lower panel: Day-by-day residual Doppler extrapolated values of 323 Stark- and second-order-Doppler-compensated line position determinations. The dashed line is the weighted mean of all 16 days. The pink lines indicate the standard deviation (940 kHz) and the blue area the standard error of the mean (410 kHz). This is thus the combined uncertainty of the residual first-order Doppler shift and the statistical error.

The intervals between the $GK(0,2)$ state and 14 members of the $nf0_3(0)$ Rydberg series with n values between 40 and 80 were recorded using single-mode continuous-wave near-infrared radiation from a Ti:sapphire laser, referenced to a frequency comb, intersecting a pulsed skimmed supersonic beam of pure H_2 emanating from a cryogenic pulsed valve. Compensating stray electric fields in three dimensions, shielding magnetic fields, and canceling the first-order Doppler shift enabled the determination of transition frequencies with uncertainties ranging from 33 kHz at $n = 50$ to 490 kHz at $n = 80$. We included a scaled systematic uncertainty of $\sigma_{n,\mathrm{dc}} = 18 \times (n/50)^7$ kHz, based on the value for $n = 50$, to account for possible dc-Stark shifts resulting from stray electric fields. We refer to Ref. [40] for further details concerning the determination of experimental uncertainties.

The binding energy of the $GK(0,2)$ state was determined by MQDT-assisted extrapolation of the $nf0_3(0)$ series in a fit where we adjusted the Hund's case (d) effective quantum defect [26]. We found that the adjustment was on the order of 10^{-5}, i.e., within the error limits given in Ref. [23]. Because the $N^+ = 0$ ion core is structureless, most of the observed $nf0_3(0)$ Rydberg states have pure singlet ($S = 0$) character [31]. The $nf0_3(0)$ levels located in the immediate

TABLE I. Overview of energy intervals used in the determination of the ionization and dissociation energies and the ortho-para separation of H_2. The values in parentheses in the second column represent the uncertainties (1 standard deviation) in the last digit. These uncertainties are given in kHz in the third column.

	Energy level interval	Value (cm^{-1})	Uncertainty (kHz)	Reference
(1)	$GK(v=1,N=2)-X(v=0,N=0)$	111 827.741 986(21)	630	This work
(2)	$GK(v=1,N=2)-GK(v=0,N=2)$	134.008 348 5(22)	66	[33]
(3)	$X^+(v^+=0,N^+=0)-GK(v=0,N=2)$	12 723.757 461(23)	700	This work
(4)	$E_I^{\text{para}}(H_2)=(1)-(2)+(3)$	124 417.491 098(31)	940	This work
(5)	$E_I^{\text{ortho}}(H_2)$	124 357.238 003(11)	340	[17]
(6)	$X^+(v^+=0,N^+=1,\text{center})-X^+(v^+=0,N^+=0)$	58.233 675 1(1) [1]	30	[34–36]
(7)	$D_0^{N^+=0}(H_2^+)$	21 379.350 249 6(6)	18	[13]
(8)	$E_I(H)$	109 678.771 743 07(10)	3	[37]
(9)	$D_0^{N=0}(H_2)=(4)+(7)-(8)$	36 118.069 605(31)	940	This work
(10)	$D_0^{N=0}(H_2)$	36 118.069 632(26)	780	[38]
(11)	$\Delta E_{\text{ortho-para}}=(4)+(6)-(5)$	118.486 770(50) [b]	1500	This work
(12)	$\Delta E_{\text{ortho-para}}$	118.486 812 7(11)	33	[38]

[a]A recent calculation by V. I. Korobov gave the value of 58.233 675 097 4(8) cm^{-1} [39].
[b]The uncertainty includes contributions of 550 kHz and 1 MHz for the experimental frequency connecting the ortho and para states of H_2^+ [12] and the theoretical uncertainty of the term values of the highest bound states of H_2^+, respectively, in addition to the uncertainties of the para- and ortho-H_2 ionization energies (assuming no anomalous effect on the para-ortho splitting).

vicinity of $n'f2_3(0)$ perturbing states represent an exception because they have mixed singlet and triplet character induced by the spin-rotation interaction in the $(v^+=0, N^+=2)$ ion core. These states were not included in the MQDT fit. The residuals of this fit are depicted in Fig. 4. We estimate the uncertainty $\delta\mu$ of the nf quantum defects to be 1.6×10^{-5}, corresponding to an uncertainty of 500 kHz at $n=60$, and to an n-dependent uncertainty $\delta\epsilon_{\text{bind}}$ in the binding energy given by

$$\delta\epsilon_{\text{bind}}/(hc)\approx\frac{2\mathcal{R}}{n^3}\delta\mu, \tag{1}$$

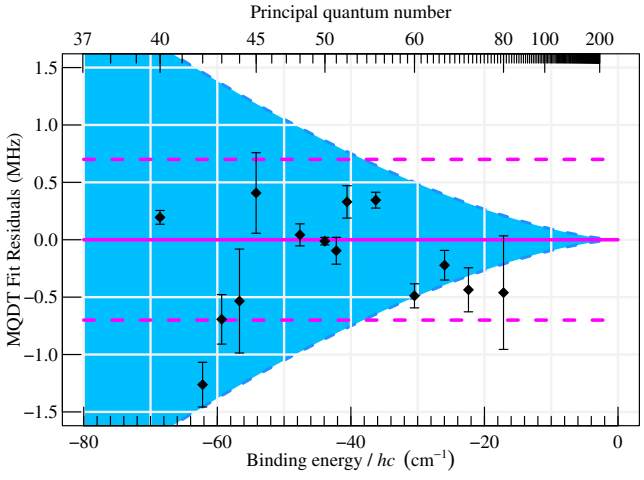

FIG. 4. MQDT fit residuals for the measured $nf0_3$ Rydberg states. The uncertainty of the binding energies of the $GK(0,2)$ state and of the high-n Rydberg states are indicated by the magenta dashed lines and the blue area, respectively.

illustrated by the blue area in Fig. 4. The extrapolated series limit corresponds to the absolute value of the binding energy of the $GK(0,2)$ state and its uncertainty of 700 kHz (1σ) is given by the dashed horizontal lines in Fig. 4. A list of the measured $nf0_3(0)$-$GK(0,2)$ intervals with corresponding experimental uncertainties and fit residuals is provided in the Supplemental Material [41].

Table I summarizes the main experimental results and all intervals needed to determine the ionization energy of para-H_2 $[E_I^{\text{para}}(H_2)=124\,417.491\,098(31)\ cm^{-1}]$, the dissociation energy of para-H_2 $[D_0^{N=0}(H_2)=36\,118.069\,605\,(31)\ cm^{-1}]$, and the interval between the ground states of ortho- and para-H_2 $[\Delta E_{\text{ortho-para}}=118.486\,770(50)\ cm^{-1}]$. The uncertainty (1σ) of $\Delta E_{\text{ortho-para}}$ includes contributions from the measurement of the $N^+=1\leftarrow N^+=0$ $(v^+=19)$ transition from Ref. [12] $(1\sigma=550$ kHz) and a conservative estimate of the uncertainty of the relevant calculated H_2^+ term values [9,11,13].

The present results were obtained in what may be referred to as a blind analysis; i.e., the intervals obtained in Amsterdam and Zurich were first determined independently with their respective uncertainties and then added for comparison with theoretical results. In this context, it is worth mentioning that the dissociation energy of ortho-H_2 reported in Ref. [38] was determined from the value of the dissociation energy of para-H_2 obtained from full four-particle nonrelativistic calculations by adding the value of $\Delta E_{\text{ortho-para}}$ calculated in the realm of nonadiabatic perturbation theory. The present values of the ionization and dissociation energies of para-H_2 thus represent a more stringent test of the theory than the $\Delta E_{\text{ortho-para}}$ value and

the dissociation and ionization energies of ortho-H_2 reported in Ref. [17].

Our value of $\Delta E_{\text{ortho-para}}$ is compatible with, but more precise than, the value of 118.486 84(10) cm^{-1} determined from the molecular constants derived from a combination of laboratory and astrophysical data on electric-quadrupole transitions of H_2 [42] (which is based on the assumption that the level structure of ortho- and para-H_2 can be described by the same constants).

$D_0^{N=0}$ (para-H_2) and $\Delta E_{\text{ortho-para}}$ both agree within the combined error bars with the theoretical values of 36118.069632(26) and 118.486 812 7(11) cm^{-1}, respectively, reported by Puchalski *et al.* [38]. Given that the first-principles calculations reported in Ref. [38] did not consider an anomalous effect on the ortho-para energy separation [43], the agreement between the experimental and theoretical values of $\Delta E_{\text{ortho-para}}$ implies an upper bound of 5×10^{-5} cm^{-1}, given by the combined uncertainty of the experimental and theoretical values, for a hypothetical global shift of the energy-level structure of ortho-H_2 with respect to that of para-H_2. This upper bound is almost 3 orders of magnitude smaller than the upper bound (780 MHz) one can derive from measurements of the dissociation energies of the $EF(0,0)$ and $EF(0,1)$ states [44].

Measurements of the dissociation energy of H_2 in para-H_2, as presented in the present work, eliminate the uncertainty related to the unresolved hyperfine structure in the X and GK (or EF) states in ortho-H_2 and thus hold the promise of a further increase in accuracy. The optimal scheme for para-H_2 would make use of a measurement of the $X(0,0)$-$EF(0,0)$ interval by Ramsey-type spectroscopy, as reported by Altmann *et al.* for the $X(0,1)$-$EF(0,1)$ interval [45]. The long lifetime of the EF $(v=0)$ levels would enable the measurement of extremely narrow transitions to high Rydberg states. Unfortunately, transitions from the EF state to nf Rydberg states have negligible intensity because the EF state has predominant $2s$ character. To nevertheless benefit from a highly accurate X-EF Ramsey-type measurement in para-H_2, we plan to use transitions to long-lived $np0_1$ Rydberg states to relate the EF and GK energies, and to use $nf0_3$-$GK(0,2)$ transitions to extrapolate to the $X^+(0,0)$ ionization limit. A similar procedure resulted in a 40 kHz relative determination of the rovibrational levels of the GK and H states [33], indicating significant potential for an even more accurate $D_0^{N=0}$ (para-H_2) value.

We thank Professor V. I. Korobov for communicating to us the result of his new calculations of the energy difference between the ground states of ortho- and para-H_2^+. F. M., W. U., and K. E. acknowledge the European Research Council for ERC-Advanced grants under the European Union's Horizon 2020 research and innovation programme (Grant Agreements No. 743121, No. 670168, and No. 695677, respectively). In addition, W. U. and K. E. acknowledge support through a program grant (16MYSTP) from FOM/NWO and F. M. acknowledges financial support from the Swiss National Science Foundation (Grant No. 200020-172620).

*Present address: Department of Physics, Yale University, New Haven, CT 06520, USA.
†Permanent address: Hefei National Laboratory for Physical Sciences at Microscale, iChem center, University of Science and Technology China, Hefei 230026, China.

[1] M. Quack, Mol. Phys. **34**, 477 (1977).
[2] D. Uy, M. Cordonnier, and T. Oka, Phys. Rev. Lett. **78**, 3844 (1997).
[3] M. Quack, in *Handbook of High-Resolution Spectroscopy*, edited by M. Quack and F. Merkt (John Wiley & Sons, Chichester, 2011), Vol. 1, pp. 659–722.
[4] T. Oka, in *Handbook of High-Resolution Spectroscopy*, edited by M. Quack and F. Merkt (John Wiley & Sons, Chichester, 2011), Vol. 1, pp. 633–658.
[5] H. Longuet-Higgins, Mol. Phys. **6**, 445 (1963).
[6] P. R. Bunker and P. Jensen, *Molecular Symmetry and Spectroscopy* (NRC Research Press, Ottawa, 2006).
[7] K. F. Bonhoeffer and P. Harteck, Naturwissenschaften **17**, 182 (1929).
[8] P. Ehrenfest and J. R. Oppenheimer, Phys. Rev. **37**, 333 (1931).
[9] R. E. Moss, Chem. Phys. Lett. **206**, 83 (1993).
[10] K. Pachucki and J. Komasa, Phys. Rev. A **83**, 042510 (2011).
[11] M. Beyer and F. Merkt, J. Chem. Phys. **149**, 214301 (2018).
[12] A. D. J. Critchley, A. N. Hughes, and I. R. McNab, Phys. Rev. Lett. **86**, 1725 (2001).
[13] V. I. Korobov, L. Hilico, and J.-P. Karr, Phys. Rev. Lett. **118**, 233001 (2017).
[14] J. Biesheuvel, J.-P. Karr, L. Hilico, K. S. E. Eikema, W. Ubachs, and J. C. J. Koelemeij, Nat. Commun. **7**, 10385 (2016).
[15] S. Alighanbari, M. G. Hansen, V. I. Korobov, and S. Schiller, Nat. Phys. **14**, 555 (2018).
[16] C.-F. Cheng, J. Hussels, M. Niu, H. L. Bethlem, K. S. E. Eikema, E. J. Salumbides, W. Ubachs, M. Beyer, N. Hölsch, J. A. Agner, F. Merkt, L.-G. Tao, S.-M. Hu, and C. Jungen, Phys. Rev. Lett. **121**, 013001 (2018).
[17] N. Hölsch, M. Beyer, E. J. Salumbides, K. S. E. Eikema, W. Ubachs, C. Jungen, and F. Merkt, Phys. Rev. Lett. **122**, 103002 (2019).
[18] J. Liu, E. J. Salumbides, U. Hollenstein, J. C. J. Koelemeij, K. S. E. Eikema, W. Ubachs, and F. Merkt, J. Chem. Phys. **130**, 174306 (2009).
[19] D. Sprecher, C. Jungen, and F. Merkt, J. Chem. Phys. **140**, 104303 (2014).
[20] P. Borrell, P. M. Guyon, and M. Glass-Maujean, J. Chem. Phys. **66**, 818 (1977).
[21] J. Zs. Mezei, I. F. Schneider, M. Glass-Maujean, and Ch. Jungen, J. Chem. Phys. **141**, 064305 (2014).
[22] D. Sprecher, M. Beyer, and F. Merkt, Mol. Phys. **111**, 2100 (2013).

[23] A. Osterwalder, A. Wüest, F. Merkt, and Ch. Jungen, J. Chem. Phys. **121**, 11810 (2004).
[24] U. Fano, Phys. Rev. A **2**, 353 (1970); **15**, 817(E) (1977).
[25] G. Herzberg and Ch. Jungen, J. Mol. Spectrosc. **41**, 425 (1972).
[26] C. Jungen, in *Handbook of High-Resolution Spectroscopy*, edited by M. Quack and F. Merkt (John Wiley & Sons, Chichester, 2011), Vol. 1, pp. 471–510.
[27] H. Gao and C. H. Greene, Phys. Rev. A **42**, 6946 (1990).
[28] M. Beyer, N. Hölsch, C. Jungen, and F. Merkt (to be published).
[29] J. J. Kay, S. L. Coy, B. M. Wong, C. Jungen, and R. W. Field, J. Chem. Phys. **134**, 114313 (2011).
[30] R. G. Neuhauser, K. Siglow, and H. J. Neusser, J. Chem. Phys. **106**, 896 (1997).
[31] C. Haase, M. Beyer, C. Jungen, and F. Merkt, J. Chem. Phys. **142**, 064310 (2015).
[32] S. Yu and K. Dressler, J. Chem. Phys. **101**, 7692 (1994).
[33] N. Hölsch, M. Beyer, and F. Merkt, Phys. Chem. Chem. Phys. **20**, 26837 (2018).
[34] V. I. Korobov, Phys. Rev. A **74**, 052506 (2006).
[35] V. I. Korobov, Phys. Rev. A **73**, 024502 (2006).
[36] V. I. Korobov, Phys. Rev. A **77**, 022509 (2008).
[37] P. J. Mohr, D. B. Newell, and B. N. Taylor, J. Phys. Chem. Ref. Data **45**, 043102 (2016).
[38] M. Puchalski, J. Komasa, P. Czachorowski, and K. Pachucki, Phys. Rev. Lett. **122**, 103003 (2019).
[39] V. I. Korobov (private communication).
[40] M. Beyer, N. Hölsch, J. A. Agner, J. Deiglmayr, H. Schmutz, and F. Merkt, Phys. Rev. A **97**, 012501 (2018).
[41] See Supplemental Material at http://link.aps.org/supplemental/10.1103/PhysRevLett.123.163002 for a list of the measured $nf0_3(0) - GK(0,2)$ transition frequencies of H_2 with corresponding experimental uncertainties and fit residuals.
[42] D. E. Jennings, S. L. Bragg, and J. W. Brault, Astrophys. J. **282**, L85 (1984).
[43] M. P. Ledbetter, M. V. Romalis, and D. F. Jackson Kimball, Phys. Rev. Lett. **110**, 040402 (2013).
[44] Y. P. Zhang, C. H. Cheng, J. T. Kim, J. Stanojevic, and E. E. Eyler, Phys. Rev. Lett. **92**, 203003 (2004).
[45] R. K. Altmann, L. S. Dreissen, E. J. Salumbides, W. Ubachs, and K. S. E. Eikema, Phys. Rev. Lett. **120**, 043204 (2018).